Received: 30 August 2022 | Revised: 16 February 2023 | Accepted: 1 March 2023

DOI: 10.1002/mp.16404

RESEARCH ARTICLE

MEDICAL PHYSICS

Choroidal neovascularization removal with photo-mediated ultrasound therapy

Mingyang Wang[1] | **Van Phuc Nguyen**[2] | **Rohit Singh**[3] | **Basheer Mossallam**[1] | **Xinmai Yang**[3] | **Xueding Wang**[1] | **Yannis M. Paulus**[1,2]

[1]Department of Biomedical Engineering, University of Michigan, Ann Arbor, Michigan, USA

[2]Department of Ophthalmology and Visual Sciences, University of Michigan, Ann Arbor, Michigan, USA

[3]Institute for Bioengineering Research and Department of Mechanical Engineering, University of Kansas, Lawrence, Kansas, USA

Correspondence
Xinmai Yang, University of Kansas, Learned Hall, Lawrence, KS 66045, USA.
Email: xmyang@ku.edu

Xueding Wang, University of Michigan, 2200 Bonisteel Boulevard, Ann Arbor, MI 48109, USA.
Email: xdwang@umich.edu

Yannis M. Paulus, University of Michigan, 1000 Wall St, Ann Arbor, MI, 48105, USA.
Email: ypaulus@med.umich.edu

Funding information
NIH, Grant/Award Numbers: R01EY029489, R41EY031219, K08EY027458; Alcon Research Institute Young Investigator Grant; Helmut F. Stern Career Development Professorship in Ophthalmology and Visual Sciences; Alliance for Vision Research; Research to Prevent Blindness; National Eye Institute, Grant/Award Number: P30 EY007003

Abstract

Background: Age-related macular degeneration (AMD) is a major cause of irreversible central vision loss. The main reason for lost vision due to AMD is choroidal neovascularization (CNV). In the clinic, current treatments for CNV include photodynamic therapy, laser photocoagulation, and anti-vascular endothelial growth factor (VEGF) therapy.

Purpose: This study evaluates a novel treatment technique combining synchronized nanosecond laser pulses and ultrasound bursts, namely photo-mediated ultrasound therapy (PUT) as a potential treatment method for CNV, for its efficacy and safety in the treatment of CNV via the experiments in a clinically-relevant rabbit model in vivo.

Methods: CNV was created by subretinal injection of Matrigel and vascular endothelial growth factor (M&V) in 10 New Zealand white rabbits. Six rabbits were used in the PUT group. In the control groups, two rabbits were treated by laser-only, and two rabbits were treated by ultrasound-only. The treatment efficacy was evaluated through fundus photography and fluorescein angiography (FA) longitudinally for up to 4 weeks. Rabbits were sacrificed for histopathology 3 months after treatment to examine the safety of PUT.

Results: The fluorescein leakage on FA was quantified to longitudinally evaluate treatment outcome. Compared with baseline, the relative intensity index was reduced by 26.57% $\pm$ 8.66% at 3 days after treatment, 27.24% $\pm$ 6.21% at 1 week after treatment, 27.79% $\pm$ 2.61% at 2 weeks after treatment, and 32.12% $\pm$ 3.23% at 4 weeks after treatment, all with a statistically significant difference of $p < 0.01$. The comparison between the relative intensity indexes from the two control groups (laser-only treatment and ultrasound-only treatment) did not show any statistically significant difference at all time points. Safety evaluation at 3 months with histopathology demonstrated that the PUT did not result in morphologic changes to the neurosensory retina.

Conclusions: This study introduces PUT for the first time for the treatment of CNV. The results demonstrated good efficacy and safety of PUT to treat CNV in a clinically-relevant rabbit model. With a single session of treatment, PUT can safely reduce the leakage of CNV for at least 1 month after treatment.

KEYWORDS
age-related macular degeneration, choroidal neovascularization, photo-mediated ultrasound therapy, PUT, retinal laser, ultrasound

1 | INTRODUCTION

Age-related macular degeneration (AMD) is a leading cause of vision loss, affecting 10% of people above 65 years old and more than 25% of people above 75 years old.[1,2] It can be classified into dry AMD (drusen, pigmentary changes, atrophy) and wet AMD (neovascular).[3] While dry AMD accounts for most diagnosed cases, wet AMD is responsible for most of the severe vision loss.[4] Approximately 10%–20% of patients with dry AMD develop the wet form, which affects 1.75 million people in the United States,[5] and is expected to increase with the aging of the population.

The main manifestation of wet AMD is choroidal neovascularization (CNV).[6,7] CNV is unstructured, leaky angiogenic vessels and is the main cause of vision loss from macular degeneration.[8] Current treatments of CNV are primarily focused on inhibiting vascular endothelial growth factor (VEGF).[9] However, the procedure used in this treatment is less than ideal because patients receiving anti-VEGF therapy require frequent (often monthly) eye (intravitreal) injections. Despite anti-VEGF therapy, 20% of patients become legally blind and another 30% suffer from some degree of vision loss after 5 years of anti-VEGF therapy.[10,11] This paper evaluates a novel technique, namely photo-mediated ultrasound therapy (PUT), which holds potential for the treatment of CNV.

PUT is a non-invasive, particle-free treatment method that incorporates both ultrasound bursts and laser pulses by synchronizing them spatially and temporally in a target area for treatment.[12] The treatment effect of PUT is based on the controlled cavitation activity.[13] Cavitation is the formation and collapse of bubbles in a liquid medium.[14] Acoustically induced cavitation activities are well known in histotripsy and anti-vascular ultrasound therapy (AVUT). In these methods, by using high intensity focused ultrasound (HIFU), cavitation could be initiated in the focal region of an ultrasound transducer when sufficient tension was caused by negative pressures, and the subsequent ultrasonic excitation will drive the formed bubbles to collapse and produce strong shock waves.[15]

PUT, on the other hand, combines the aforementioned acoustic cavitation with laser pulses, which introduces a mechanism called photoacoustic (PA) cavitation.[12,16] The PUT working mechanism mainly consists of two phases. In the first phase, the bubble nucleates in the target vessel due to irradiation of a nanosecond laser pulse at one of the peak negative pressures of an ultrasound burst. In the second phase, the nucleated bubble is driven by the subsequent ultrasound cycle of the burst to produce cavitation inside a blood vessel. Compared with the cavitation induced by HIFU-only, in PUT, the cavitation pressure threshold also depends on the optical parameters, such as the size of the optically absorptive target, the optical absorption coefficient of the target, and the fluency of the applied laser pulse. Benefiting from its distinctive mechanism, PUT can provide better vessel selectivity by taking advantage of the optical absorption contrast in biological tissues[17] while producing a treatment effect by using acoustic energy much less than that needed by HIFU-only therapy.[18]

In our previous study, the anti-vascular effect of PUT has been studied in several different contexts, including subcutaneous vessels,[19] choroidal vessels,[20] corneal neovascularization,[21] and retinal neovascularization.[22] Furthermore, we have tested and examined the characteristics of a clinically-relevant New Zealand white (NZW) rabbit CNV model.[2] Based on these previous works, in this study, we evaluated the potential of PUT for CNV treatment via the experiments on the clinically relevant rabbit CNV model in-vivo.

2 | METHODS

2.1 | Ultrasonic components

A PUT system capable of delivering the required ultrasonic and optical excitation into the rabbit's eye was developed, as shown in Figure 1. Figure 1a shows a photograph of the system. The therapeutic ultrasound system, as shown in the schematic in Figure 1b, has been well described in a previous publication.[22] This system contains a function generator (DS345, Stanford Research System, Sunnyvale, CA), a power amplifier (2100L, ENI, Rochester, NY), an impedance matching network (Impedance Matching Network H-117, Sonic Concepts, Bothell, WA), and a HIFU transducer (0.25 MHz center frequency, 6.04 mm focal width, 39.49 mm focal length, H-117, Sonic Concepts, Bothell, WA). A cone shape coupling media made of agar gel was attached to the transducer surface. The shape of the coupling gel cone was based on the transducer's geometric ultrasound field with a hole reserved in the center for the light path. The end of the coupling gel cone contacting the eye was made spherically concave to best fit the curvature of the cornea. The quality of the acoustic coupling was verified by monitoring the PA signals produced from the eye fundus and received by the HIFU transducer.

2.2 | Optical components

The layout of the optical components used for PUT at the fundus of the rabbit eye is shown in Figure 1e. As previously reported,[22] a Nd:YAG laser (Continuum DLS 8010 Powerlite, Santa Clara, CA) was used to emit the treatment light at 1064 nm, and the residual 532 nm light was subsequently eliminated. The 1064 nm light was focused to a 6 mm spot before the rabbit eye by an objective lens with 19 mm focal length (divergence half angle = 10.437°, AC127-019-AB-ML,

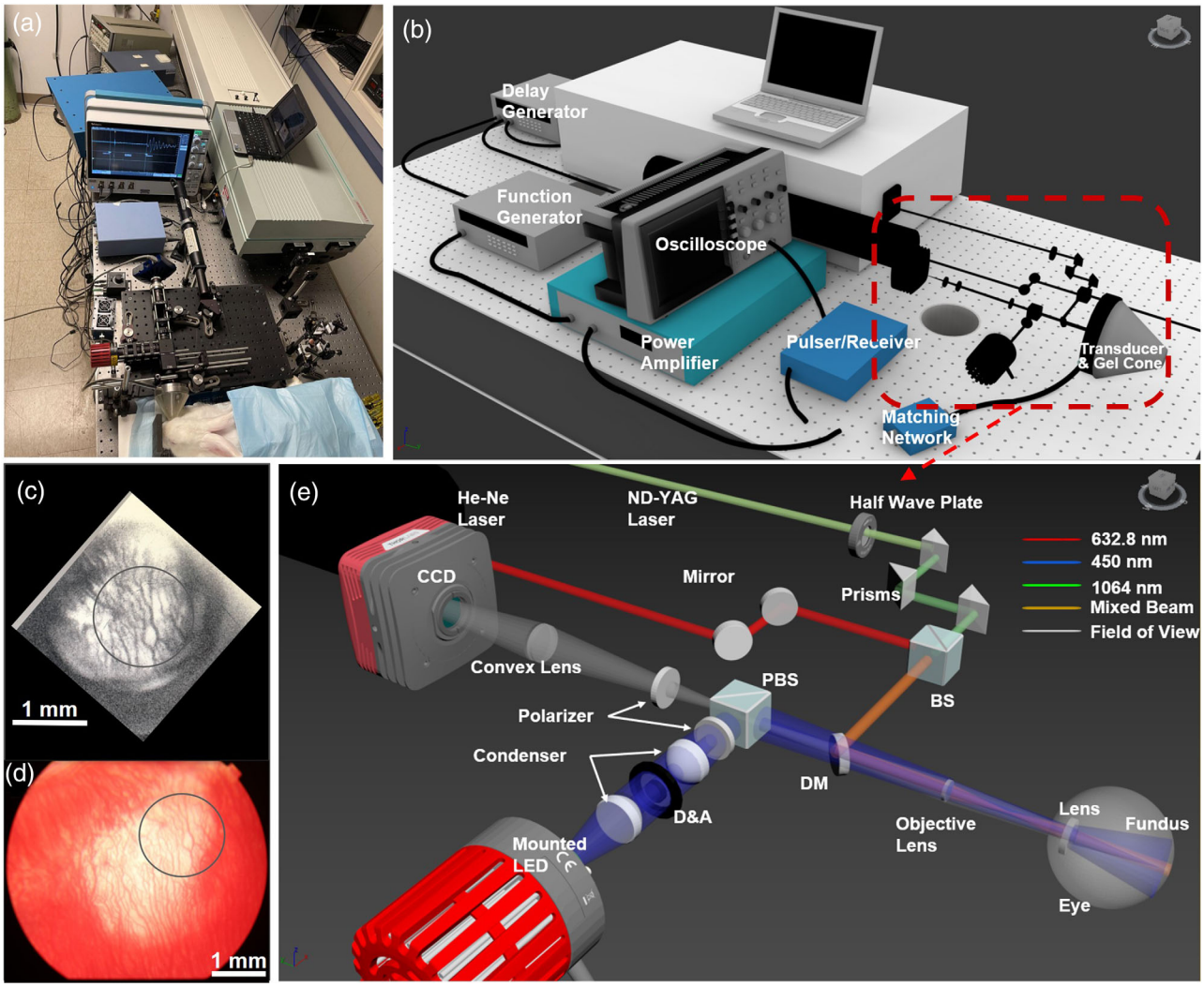

FIGURE 1 PUT system for treatment of CNV in a rabbit eye in vivo. (a) Shows a photograph of the system. (b) Shows the schematic of the overall system. (c) and (d) Show example photographs of the eye fundus captured during the treatment, where (c) was taken with a CCD camera and (d) was taken with a Topcon 50EX Fundus Camera and Olympus DP70 digital camera system. (e) Shows the design of the optical path red-circled in (b). PBS, polarize beam splitter; BS, beam splitter; DM, dichroic mirror; D&A, diffuser with annulus cover; CCD, charge-coupled device.

Thorlabs). By using an enucleated rabbit eye and a near-infrared detector card placed on the fundus, the laser spot size at the fundus was directly quantified as 3 mm in diameter. The illumination and visualization of the fundus were provided by a charge coupled device (CCD) and a mounted LED. The illumination light beam first passed through two aspheric condenser lenses with a diffuser surface. Between the two condenser lenses, an obstruction target with an annular aperture was placed to make the illumination light as a ring shape. The ring-shape illumination light then passed through a polarizing beam-splitter (PBS) and was finally focused on the rabbit eye. A HeNe laser (wavelength 632.8 nm, HNL020LB, Thorlabs) generated a guiding beam that was used to identify the treatment location on the retina through the CCD.

2.3 | Acoustic and optical synchronization

The delay generator shown in Figure 1b (DG535, Stanford Research System, Sunnyvale, CA) simultaneously triggered the laser and ultrasonic components, synchronizing them at a repetition rate of 10 Hz. Before each treatment, the laser was turned on, and the HIFU transducer was in the receive mode (by connecting the matching network to the pulse receiver shown in Figure 1b). The fundus PA signal received by the HIFU transducer was amplified by the pulse receiver and then shown on the oscilloscope. The HIFU transducer's position, held by a 3D stage, was adjusted to find the position where the detected PA signal amplitude was maximal, which ensured the spatial synchronization. The

PA signal's traveling time from the fundus to the transducer was measured on the oscilloscope. Using the time-reversal method described in earlier work,[23] the measured traveling time was used to modify the delay on the delay generator setting to guarantee that the laser and ultrasound were also temporally synchronized. Only one laser pulse was fired on the target at the start of each ultrasound burst, synchronizing with the negative peak of the ultrasonic cycle, whereas each HIFU burst had 2500 cycles at 0.25 MHz

2.4 | Acoustic and optical delivery

Prior to reaching the ocular surface, the laser energy employed in this study was calibrated and measured to be 10 mJ. The laser fluence at the target was calculated to be 85 mJ/cm^2, considering the laser beam size of 3 mm in diameter and 40% attenuation before the 1064 nm light reached the retinal layer.[22] The HIFU transducer was on transmit mode (by connecting the matching network to the power amplifier shown in Figure 1b) during the treatment. The fundus was exposed to a 0.25 MHz, 2500 cycle ultrasound at a pressure of 0.36 MPa negative peak, calibrated using a needle transducer in an eye of a euthanized rabbit. The treatment response was anticipated to occur in the laser focal region (3 mm in diameter) which was covered by the HIFU focal region (6 mm in diameter). The total treatment time for each rabbit eye was 5 min.

2.5 | In vivo CNV model

Ten NZW rabbits (weight 2.5–3.5 kg, 2–9 months of age, both male and female) received subretinal injection of Matrigel and vascular endothelial growth factor (M&V). M&V suspension was prepared by suspending 750 ng human VEGF-165 (Shenandoah Biotechnology, Warwick, USA) (100 μg/mL) in 20 μL Matrigel basement membrane matrix (Corning, NY, USA) as described previously.[2] The injection location was modified to be at the center of fundus right next the central horizontal medullary ray. All rabbits were observed weekly for at least 2 weeks after injection. The PUT was then performed 2 weeks after the subretinal fluid had been cleared and hyperfluorescence could be observed at the injection area.

2.6 | Quantification method and statistical analysis

To evaluate the PUT effect, changes of CNV intensity at different observation time points were evaluated by quantitively study the late phase leakage area in fluorescein angiography. Figure 2 shows an example to demonstrate the control points match method that was used to align images taken at different times. This was done by labeling 8–10 common landmarks such as distinctive choroidal and retinal blood vessels and the optic nerve in both images to determine the position information. The position index of these common points was used for inferring a geometric transformation that aligned the control points (Figure 2a). Once aligned, the region of interest would be shown on the exact same pixel location on each image (Figure 2b). Considering the PUT effect would only occur inside the laser focus area, the CCD image acquired during the treatment was first aligned with the fundus image before treatment. As aforementioned, a HeNe laser was used to illuminate the treatment area. Once the CCD image and fundus image were aligned, the edge of the red light could be circled as the treatment area on each image (Figure 2c).

Considering the fluorescein leakage is a key feature of CNV, the hyperintensity of each image was first extracted by setting the median of intensity as binary threshold. The histogram of such fluorescence photo with a hyperfluorescence area is shown in Figure 3a. These histograms typically have two peaks, with the high intensity peak labeled in Figure 3a corresponding to the hyperfluorescence area. For each eye, the FA images taken at different observation time points were histogram matched with the FA image before treatment to ensure they were scaled similarly. For each eye, an optimal intensity level was chosen as the threshold to convert the FA images into the binary images with the hyperfluorescence area shown in white and the normal fluorescence area shown in black (Figure 3b1–b2). The white area in a binary image (i.e., hyperfluorescence area) was considered to be the "leakage area." Another binary image showing the "mask" of the treatment area is in Figure 3c1–c2. To quantify the mean intensity level inside the treatment area and its change in respond to treatment, we calculated the "Relative Intensity Index" using the following equation:

$$\textit{Relative Intensity Index} = \frac{\textit{Mean Intensity in Treatment area}}{\textit{Mean Intensity in Leakage area}}$$

To study the changes in fluorescence leakage in the eyes at each of the post-treatment observation time points when compared to the before-treatment measurement, un-paired *t*-tests were conducted. The differences were considered statistically significant when p values were less than 0.01.

2.7 | Histology and immunohistochemistry

Three NZW rabbits were euthanized at 3 months after PUT through a lethal dose of pentobarbital. The eyes were harvested immediately and pre-fixed in

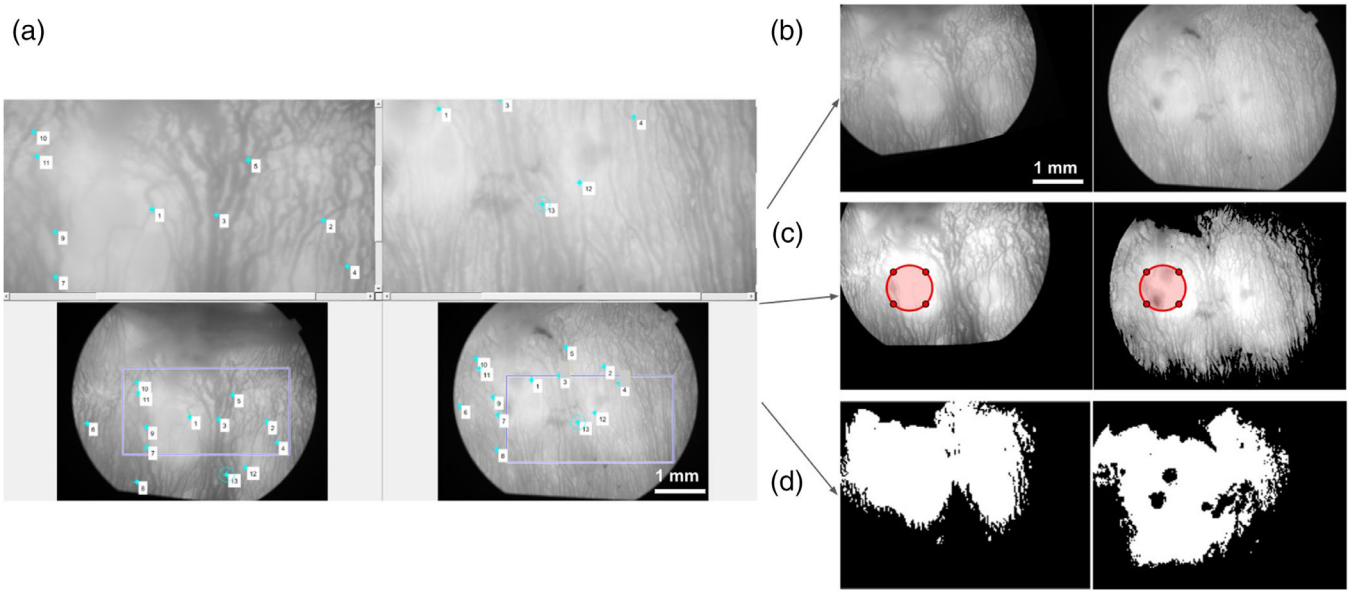

FIGURE 2 (a) Shows the same "landmarks" are selected between two images as the control points. (b) Unregistered image pair taken at two different observation time points. (c) Registered image pair. The red circles mark the treatment area. (d) Hyperfluorescence part extracted showing the CNV leakage area.

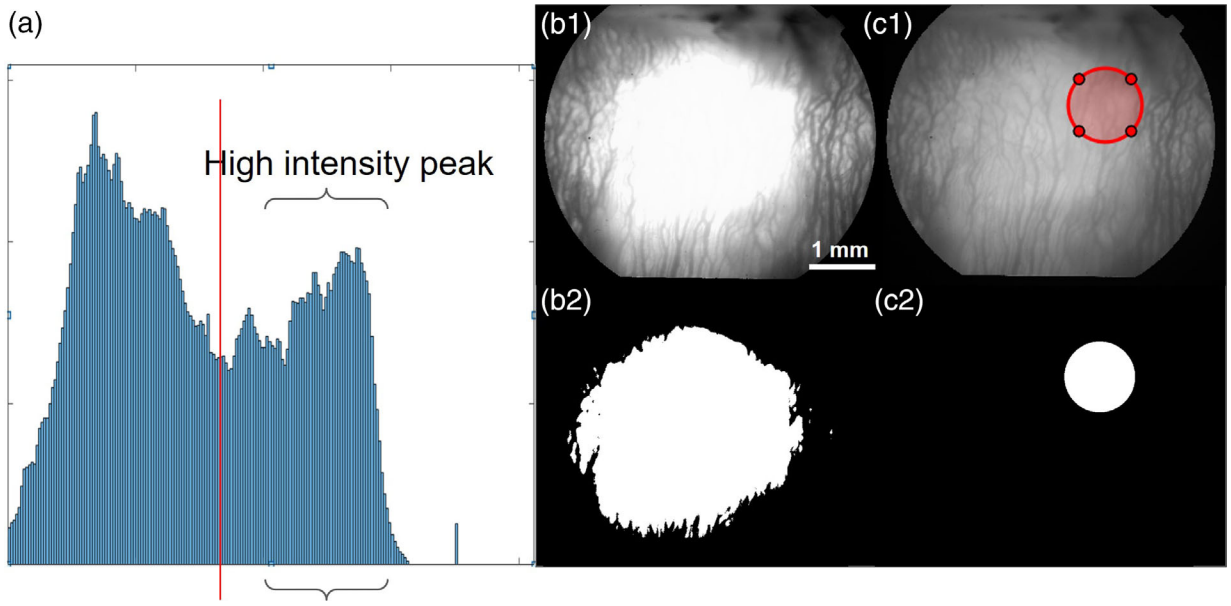

FIGURE 3 (a) Pixel intensity histogram of a representative FA late phase image shown in (b1). The red line marks the binary threshold. (b2) Binary result of (b1), indicating the leakage area. (c1) Original FA late phase photo with the treatment area labeled by the red circle. (c2) Binary image showing the treatment area.

10% formalin solution for 24 h. The fixed eyes were then changed to 50% ethanol for 8 h and then 70% ethanol for 24 h. The eyes were split and the strips containing treatment area were fixed in 4% agar then embedded in paraffin. The paraffin-embedded sections were finally sliced and stained by hematoxylin and eosin (H&E) or Smooth Muscle Actin (SMA) antibody.

3 | RESULTS

3.1 | Efficacy of PUT

In total, six NZW rabbits (left eye in each rabbit) with CNV model were treated with a single PUT session. Representative PUT results are shown in Figure 4; while the other results are shown in Figures S1–S5. Control

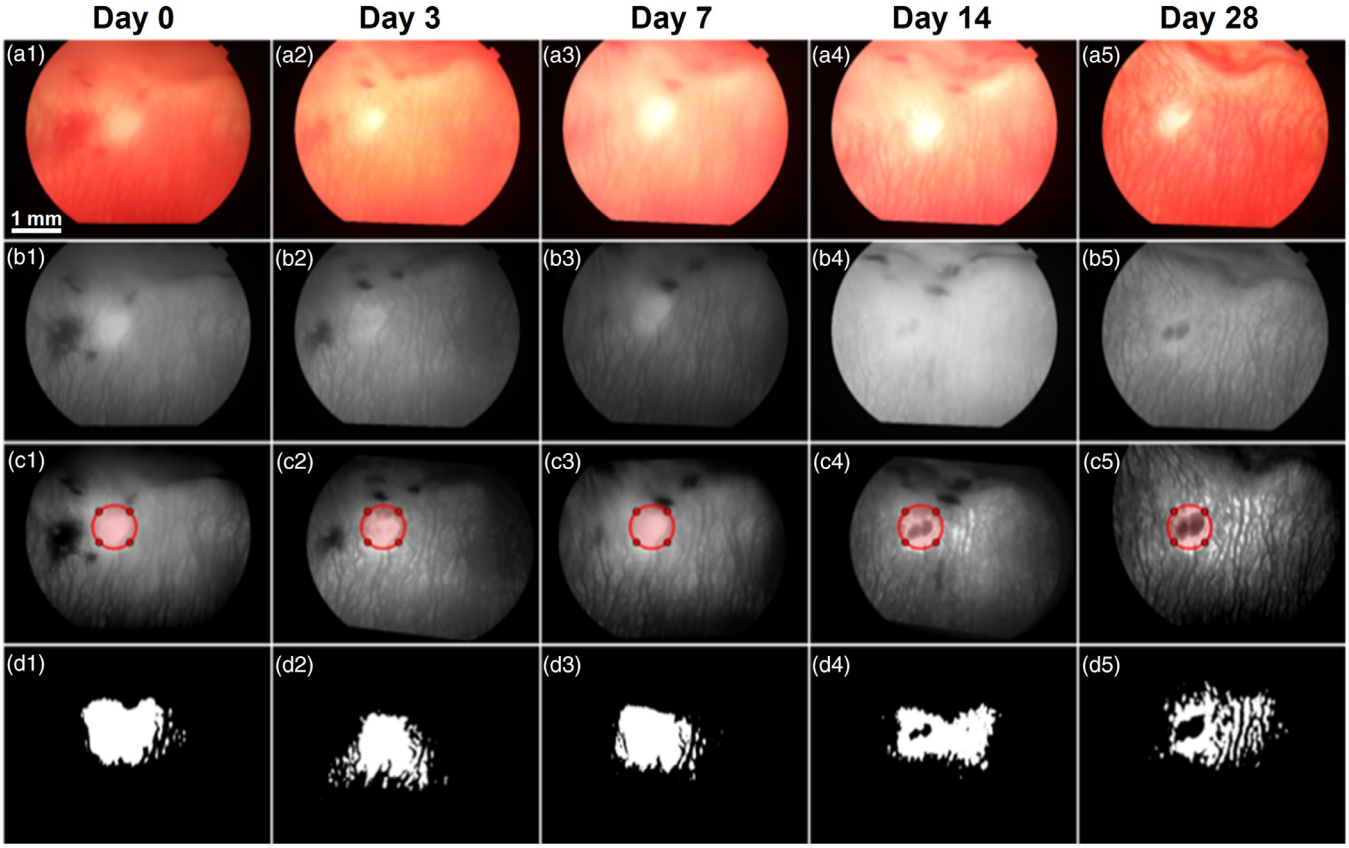

FIGURE 4 Representative PUT result in a rabbit CNV model. (a1–a5) Fundus photographs and (b1–b5) late phase FA images taken at different observation time points, including Day 0 (immediately before PUT treatment and 2–4 weeks after M&V injection), and Day 3, Day 7, Day 14, and Day 28 after the treatment. (c1–c5) Registered late phase FA images at different observation time points, where the red circles indicate the treatment area. (d1–d5) Binary images at different observation time points, showing the hyperfluorescent area consistent with the CNV leakage.

experiments with laser-only and ultrasound-only treatments were also conducted. Two NZW rabbits (left eye in each rabbit) with CNV model were treated by laser only with the same optical parameters (10 Hz 1064 nm laser pulse with 140 mJ/cm^2 laser fluence for 5 min). Two NZW rabbits (left eye in each rabbit) with CNV model were treated by ultrasound only with the same ultrasound parameters (0.36 MPa ultrasound pressure at 0.25 MHz with 2500 cycle each burst, 10 Hz burse repetition rate for 5 min).

At each observation time point, the fundus photo and FA images were captured. In Figure 4 and Figures S1–S5, the representative fundus images are shown on the first row (**A1–A5**), the original and the registered figures of late phase of FA images are shown on the second and third rows, respectively (**B1–B5** and **C1–C5**), and the extracted hyperfluorescent area are shown on the fourth row (**D1–D5**). On Day 0, the FA late phase showed hyperfluorescent areas which were induced by vessel leakage overlying on the choroidal vessels, indicating the existence of CNV. Immediately after treatment, microhemorrhages within the treatment area were noted. Due to their optical absorption of the fluorescent light, the areas covered by these microhemorrhages may show hypofluorescent blockage in the fundus FA image. These microhemorrhages were fully absorbed within the following 3 days in all six cases. After that, the reduced hyperfluorescence in the treatment area indicates that the neovasculature treated by PUT have either stopped perfusion or the vessel structure was removed by PUT. In addition, we also notice that the reduction in hyperfluorescence is heterogeneous in the treatment area, which reflects that the vascular response to the PUT is not homogenous.

For each rabbit eye in the PUT group or the control groups, the treatment efficiency was evaluated longitudinally by quantifying the fluorescein leakage in fluorescein angiography. Using the measurements on Day 0 (before treatment) as a baseline, the average and the 95% confidence interval of the quantified relative intensity index of the three groups (PUT, laser-only treatment, and ultrasound-only treatment) at each time point are shown in Figure 5. One time PUT can effectively reduce the fluorescence leakage of CNV, as reflected by the reduction in the relative intensity index, of 26.57% ± 8.66% on Day 3, 27.24% ± 6.21% on Day 7, 27.79% ± 2.61% on Day 14, and 32.12% ± 3.23%

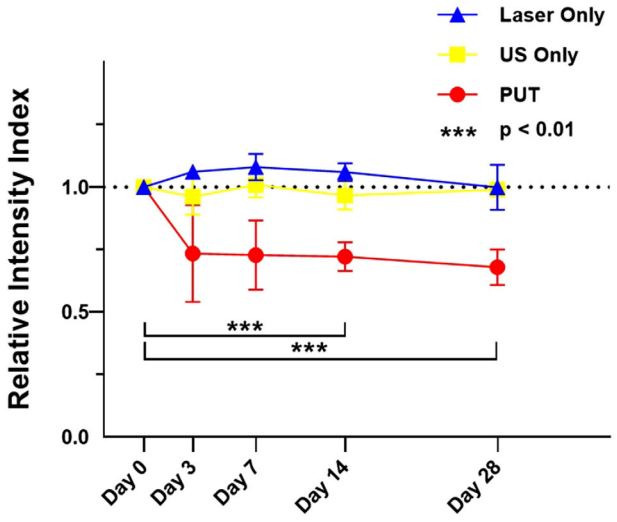

FIGURE 5 Quantification of the relative intensity index as a function of time after PUT ($n = 5$), ultrasound (US) only treatment ($n = 2$), and laser only treatment ($n = 2$). For the PUT group, the average reduction in relative intensity index is 26.57% ± 8.66% on Day 3, 27.24% ± 6.21% on Day 7, 27.79% ± 2.61% on Day 14, and 32.12% ± 3.23% on Day 28; the quantified measurements of the relative intensity index on Days 14 and 28 show statistically significant difference when comparing to the baseline (Day 0). For the two control groups (United States only and laser only), no statistically significant change is noticed after the treatment. **** indicates p-value < 0.0001.

on Day 28. Paired t-tests comparing the quantified relative intensity indices in the treatment area on Days 14 and 28 after treatment with the baseline (Day 0; before treatment) show statistically significant differences with $p < 0.01$. For the two control groups (laser-only and ultrasound-only), no statistically significant changes in fluorescence leakage in the treatment areas was noticed at any of the observation time points after the treatment.

3.2 | Safety of PUT

Three New Zealand white rabbits were kept until 3 months after treatment for safety evaluation. H&E histology staining was performed to evaluate possible damage to the fundus structure, and α-SMA brightfield staining was performed to enhance the visualization of capillaries. For all three rabbits, every single eyecup was sliced as cross section with each slide being 200 microns apart. These slides contained three typical areas: area without CNV model, area with CNV model then treated by PUT, and area with CNV model but no treatment.

Representative histology and immunohistochemistry results were shown in Figure 6. Histology photos with H&E stains (Figure 6d–f) of the retina of these rabbits demonstrate retinal atrophy and thinning. Although every retina layer exists, significant thinning of these layers can be noticed. The retina atrophy and thinning shown by the H&E histology were caused by subretinal injection, like the results of DL-AAA model published previously.[22] No significant additional changes were induced by the PUT. The immunohistochemistry results shown in Figure 6a–c better demonstrate the irregular vascular structures. The a-SMA stain, which helps further separate RPE layer from vascular structures, also helps distinguish irregular density and thickness of vascular in the sub-retinal layer. In Figure 6a,d, the existence of macrophage cells is observed, further validating the existence of CNV. Overall, the histology and immunohistochemistry results demonstrated that PUT did not result in visible morphologic changes in the neurosensory retina.

4 | DISCUSSION

4.1 | Selection of PUT parameters

PUT relies on both laser and ultrasonic parameters because of its unique mechanism of action. The current study selected laser and ultrasound parameters based on our previous study on PUT of retinal neovascularization.[22] In the future, further optimization of the laser and ultrasonic parameters will be performed.

During PUT, only one laser pulse was fired on the target at the beginning of each ultrasound burst to induce cavitation. Due to the fact that it takes two ultrasound cycles for the response of the HIFU transducer to reach the steady state and produce the calibrated pressure, the laser pulse was synchronized with the third peak rarefaction phase of the HIFU burst. Since the 0.25 MHz HIFU transducer was operated at 10% duty cycle (2500 cycles for each burst), the 2497 subsequent ultrasound pulses kept driving the formed bubbles in vessels. Our previous study[23] has demonstrated that the efficiency of PUT can be significantly improved for vessel treatment when the laser pulse is synchronized with the HIFU rarefaction phase. We had also demonstrated that the proper synchronization can significantly enhance the cavitation effect during PUT.[16]

Unlike our group's previous studies which used a 0.5 MHz center-frequency HIFU transducer for treatment, this study utilized a 0.25 MHz transducer. This change was made because the lower frequency could provide a larger focus zone and a lower cavitation threshold due to the increase in the period of the rarefactional phase.[13] Moreover, the larger ultrasound beam could provide a more flexible angle for eye treatment. While the lens in the eye does not affect the ultrasound propagation, it does affect the focusing of incident laser light on the fundus due to refraction. Since PUT is based on spatially aligned ultrasound focus and laser focus, misalignment may be induced by refraction of the treatment laser beam. By using an ultrasound beam that is

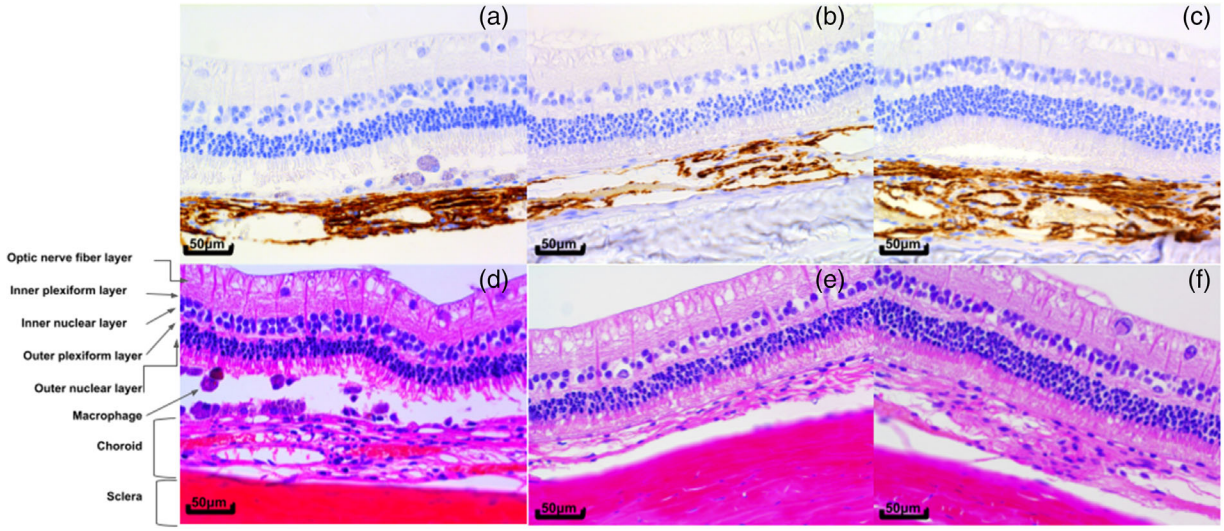

FIGURE 6 Representative histopathology results demonstrating the treatment effect and safety. (a) and (d) H&E histology and immunohistochemistry photos taken from an area with CNV model. (b) and (e) H&E histology and immunohistochemistry photos taken at 3 months after PUT, showing CNV removed in the treatment area. (c) and (f) H&E histology and immunohistochemistry photos of normal area. Both (a), (d) and (b), (e) show retinal atrophy due to the M&V subretinal injection model. However, no difference is noted between the regions of PUT area and untreated area, demonstrating no additional effect to the retina caused by PUT.

four times larger than the laser beam in diameter, it is less challenging to ensure the laser beam is within the focus zone of the HIFU beam.

4.2 | Characteristics and treatment response of M&V induced CNV model

The CNV model in this study was similar to the CNV found in age-related macular degeneration (AMD) patients in terms of fluorescein angiography leakage patterns.[24] The CNV leakage area is best visualized with stronger contrast between the CNV area and the surrounding normal area on the late-phase fluorescein angiography (FA) since there is continued leakage throughout the angiogram duration in the region of CNV. The half-life of fluorescein in extravascular tissue is longer than that of intravascular fluorescein, and thus the early removal of intravascular fluorescein results in higher signal (through continued leakage in the region of CNV) and reduced noise (through reduction in intravascular fluorescein) in the late phase FA. Despite strictly controling the M&V concentration, volume, and location of injection, the final developed CNV model varies in each eye. To account for this difference, this study utilizes a relative intensity index to account for this baseline difference between animals.

4.3 | Biological effects and biochemical changes

Besides the morphology changed shown in Figure 6, several biological effects and biochemical changes are expected during PUT. First, the endothelial cells in the CNV may become dysfunctional as a result of the enhanced cavitation during PUT. Moreover, our recent work demonstrated that endothelial cell release of the vasoactive substances NO and PGI2 may also be reduced as a result of PUT.[25]

4.4 | Unexpected treatment response

Among the 6 PUT cases, several ($n = 3$) showed treatment responses outside of the laser beam area. This may have occurred due to the downstream effects of the vasculature within the treatment area. Another possible reason is the eye movement during treatment. Although each rabbit was subjected to general anesthesia with ketamine and xylazine and topical tetracaine before treatment, spontaneous eye movement can still occur during the 5-min treatment window. These side effects may be solved by fixating the eye or updating the treatment parameters leading to reduced treatment duration.

4.5 | Limitation of current study

There are some limitations of this study. The M&V induced CNV model, while resulting in consistent, long-term persistent CNV, also shows overlying retinal atrophy which does not mimic human CNV disorders and limits the ability of this study to fully evaluate safety.[2] Since PUT relies on the bioeffects caused by cavitation bubbles, a modality that can give real-time feedback on the activities of cavitation bubbles at

the eye fundus should be developed in the future. In addition, longer follow-up can also be performed in future studies to determine the long-term treatment effect of PUT. Moreover, several modifications could be considered in the future to further optimize the PUT effect, such as introducing imaging guidance during the treatment, performing multiple treatment sessions instead of once as in this study, scanning treatment spot to cover the entire disease area, and further optimizing the optical and ultrasound parameters in PUT.

5 | CONCLUSIONS

This is the first study to explore and validate the efficacy and safety of PUT to treat CNV in a clinically-relevant rabbit model. PUT could reduce the leakage of CNV with a single treatment session, and the treatment effect persisted for at least 1 month after treatment with no damage noticed in the neurosensory retina. Despite the limitations mentioned above, PUT holds great potential to be developed into a new tool for clinical long-term management of CNV, especially for patients not responding well to anti-VEGF therapy.

ACKNOWLEDGMENTS

The authors would like to thank the generous animal donation from the Center for Advanced Models and Translational Sciences and Therapeutics at the University of Michigan and Dr. Yuqing Chen. The publication resulted from research supported by NIH R01EY029489 (X.Y.), NIH R41EY031219 (Y.M.P.), NIH K08EY027458 (Y.M.P.), the Alcon Research Institute Young Investigator Grant (Y.M.P.), the Helmut F. Stern Career Development Professorship in Ophthalmology and Visual Sciences (Y.M.P.), the Alliance for Vision Research (Y.M.P.), and Research to Prevent Blindness (Y.M.P.). This research utilized the Core Center for Vision Research funded by the National Eye Institute (P30 EY007003).

CONFLICT OF INTEREST STATEMENT

Yannis M. Paulus, Xinmai Yang, and Xueding Wang do duty as the inventors on a patent application of PUT technology from University of Kansas and University of Michigan. Yannis M. Paulus, Xinmai Yang, and Xueding Wang have equity in PhotoSonoX LLC.

REFERENCES

1. Smith W, Assink J, Klein R, et al. Risk factors for age-related macular degeneration: pooled findings from three continents. *Ophthalmology*. 2001;108(4):697-704.
2. Li Y, Zhang W, Nguyen VP, et al. Real-time OCT guidance and multimodal imaging monitoring of subretinal injection induced choroidal neovascularization in rabbit eyes. *Exp Eye Res*. 2019;186:107714.
3. Mitchell P, Liew G, Gopinath B, Wong TY. Age-related macular degeneration. *The Lancet*. 2018;392(10153):1147-1159.
4. Gheorghe A, Mahdi L, Musat O. Age-related macular degeneration. *Rom J Ophthalmol*. 2015;59(2):74-77.
5. Chou R, Dana T, Bougatsos C, Grusing S, Blazina I. Screening for impaired visual acuity in older adults: updated evidence report and systematic review for the US Preventive Services Task Force. *JAMA*. 2016;315(9):915-933.
6. Al-Zamil WM, Yassin SA. Recent developments in age-related macular degeneration: a review. *Clin Interv Aging*. 2017;12:1313-1330.
7. Grossniklaus HE, Green WR. Choroidal neovascularization. *Am J Ophthalmol*. 2004;137(3):496-503.
8. Nguyen VP, Li Y, Henry J, et al. Plasmonic gold nanostar-enhanced multimodal photoacoustic microscopy and optical coherence tomography molecular imaging to evaluate choroidal neovascularization. *ACS Sens*. 2020;5(10):3070-3081.
9. Nagai N, Ju M, Izumi-Nagai K, et al. Novel CCR3 antagonists are effective mono- and combination inhibitors of choroidal neovascular growth and vascular permeability. *Am J Pathol*. 2015;185(9):2534-2549.
10. Kovach JL, Schwartz SG, Flynn HW, Jr, Scott IU. Anti-VEGF treatment strategies for wet AMD. *J Ophthalmol*. 2012;2012:786870.
11. Scott AW, Bressler SB. Long-term follow-up of vascular endothelial growth factor inhibitor therapy for neovascular age-related macular degeneration. *Curr Opin Ophthalmol*. 2013;24(3):190-196.
12. Yang X, Paulus YM, Wang X. Antivascular photo-mediated ultrasound therapy and its application in the eye. *J Acoust Soc Am*. 2019;145(3):1810-1810.
13. Singh R, Wang XD, Yang XM. Cavitation induced shear and circumferential stresses on blood vessel walls during photo-mediated ultrasound therapy. *Aip Adv*. 2020;10(12):125227.
14. Young FR. *Cavitation*. McGraw-Hill; 1989.
15. Coussios CC, Farny CH, Haar GT, Roy RA. Role of acoustic cavitation in the delivery and monitoring of cancer treatment by high-intensity focused ultrasound (HIFU). *Int J Hyperthermia*. 2007;23(2):105-120.
16. Li S, Qin Y, Wang X, Yang X. Bubble growth in cylindrically-shaped optical absorbers during photo-mediated ultrasound therapy. *Phys Med Biol*. 2018;63(12):125017.
17. Hu Z, Zhang H, Mordovanakis A, et al. High-precision, non-invasive anti-microvascular approach via concurrent ultrasound and laser irradiation. *Sci Rep*. 2017;7(1):40243.
18. Cui H, Yang X. Laser enhanced high-intensity focused ultrasound thrombolysis: an in vitro study. *J Acoust Soc Am*. 2013;133(2):EL123-128.
19. Wang M, Qin Y, Wang T, et al. Removing subcutaneous microvessels using photo-mediated ultrasound therapy. *Lasers Surg Med*. 2020;52(10):984-992.
20. Zhang H, Xie X, Li J, et al. Removal of choroidal vasculature using concurrently applied ultrasound bursts and nanosecond laser pulses. *Sci Rep*. 2018;8(1):12848.
21. Qin Y, Yu Y, Fu J, et al. Photo-mediated ultrasound therapy for the treatment of corneal neovascularization in rabbit eyes. *Transl Vis Sci Technol*. 2020;9(13):16.
22. Qin Y, Yu Y, Fu J, et al. Photo-mediated ultrasound therapy for the treatment of retinal neovascularization in rabbit eyes. *Lasers Surg Med*. 2022;54(5):747-757.
23. Qin Y, Yu Y, Xie X, et al. The effect of laser and ultrasound synchronization in photo-mediated ultrasound therapy. *IEEE Trans Biomed Eng*. 2020;67(12):3363-3370.
24. Tomi A, Marin I. Angiofluorographic aspects in age-related macular degeneration. *J Med Life*. 2014;7(4):4-17.
25. Karthikesh MS, Wu S, Singh R, Paulus Y, Wang X, Yang X. Effect of photo-mediated ultrasound therapy on nitric oxide and

prostacyclin from endothelial cells. *Appl Sci (Basel)*. 2022;12(5): 2617.

SUPPORTING INFORMATION

Additional supporting information can be found online in the Supporting Information section at the end of this article.

How to cite this article: Wang M, Nguyen VP, Singh R, et al. Choroidal neovascularization removal with photo-mediated ultrasound therapy. *Med Phys*. 2023;50:3661–3670. https://doi.org/10.1002/mp.16404